POLITECNICO DI TORINO
Repository ISTITUZIONALE

Experimental demonstration of machine-learning-aided QoT estimation in multi-domain elastic optical networks with alien wavelengths

Original
Experimental demonstration of machine-learning-aided QoT estimation in multi-domain elastic optical networks with alien wavelengths / Proietti, R; Chen, X; Zhang, K; Liu, G; Shamsabardeh, M; Castro, A; Velasco, L; Zhu, Z; Yoo, S. J. B.. - In: JOURNAL OF OPTICAL COMMUNICATIONS AND NETWORKING. - ISSN 1943-0620. - STAMPA. - 11:1(2019), pp. A1-A10. [10.1364/JOCN.11.0000A1]

Availability:
This version is available at: 11583/2972264 since: 2022-10-12T13:49:20Z

Publisher:
Optical Society of America

Published
DOI:10.1364/JOCN.11.0000A1

Terms of use:

This article is made available under terms and conditions as specified in the corresponding bibliographic description in the repository

Publisher copyright
Optica Publishing Group (formely OSA) postprint/Author's Accepted Manuscript

"© 2019 Optica Publishing Group. One print or electronic copy may be made for personal use only. Systematic reproduction and distribution, duplication of any material in this paper for a fee or for commercial purposes, or modifications of the content of this paper are prohibited."

(Article begins on next page)

19 April 2024

Experimental Demonstration of Machine Learning-aided QoT Estimation in Multi-domain Elastic Optical Networks with Alien Wavelengths

Roberto Proietti, Xiaoliang Chen, Kaiqi Zhang, Gengchen Liu, M. Shamsabardeh, Alberto Castro, Luis Velasco, Zuqing Zhu, and S. J. Ben Yoo, *Fellow, OSA, Fellow, IEEE*

***Abstract* — In multi-domain elastic optical networks with alien wavelengths, each domain needs to consider intra-domain and inter-domain alien traffic to estimate and guarantee the required quality of transmission (QoT) for each lightpath and perform provisioning operations. This paper experimentally demonstrates an alien wavelength performance monitoring technique and machine learning-aided QoT estimation for lightpath provisioning of intra-inter-domain traffic. Testbed experiments demonstrate modulation format recognition, QoT monitoring and cognitive routing for a 160 GBd alien multi-wavelength lightpath. By using experimental training datasets from the testbed and an artificial neural network (ANN), we demonstrated an accurate optical signal to noise (OSNR) prediction with accuracy ~ 95% when using 1,200 data points.**

***Index Terms*—Multi-Domain Elastic Optical Networks, Alien Wavelength, Machine Learning.**

I. Introduction

Elastic optical networks (EON) make use of dynamic and adaptive provisioning to guarantee efficient and flexible network resources utilization. To provide the required level of flexibility and dynamicity, the network control and management plane needs automated provisioning schemes with robust quality of transmission (QoT) estimation based on the actual network link conditions. As analytical models can only offer rough estimates of the QoT of lightpaths [1], it becomes necessary to consider high margins to compensate for model inaccuracies while guaranteeing the target QoT over the duration of the lightpaths. Such high margins have a negative impact on the maximum utilization of the network capacity. Therefore, more accurate situation-aware QoT estimations are desirable.

The scenario becomes more complicated when it becomes necessary to support high-capacity and dynamic traffic demands across multiple autonomous systems (ASes) [2-4]; in this scenario, lightpaths might neither originate nor end in one single operator domain, but transparently traverse several of them. These lightpaths are known as *alien wavelengths* [5, 6]. Guaranteeing the quality-of-transmission (QoT) of end-to-end lightpaths is non-trivial across optically transparent inter-domain networks. Due to administrative constraints, each AS manager (or domain manager - DM) may disclose only very limited intra-domain information, making QoT estimation of inter-domain lightpaths challenging. As a consequence, previous QoT estimation solutions based on analytical methods [7] cannot be easily applied since they require full knowledge of the domains (i.e., topology, links characteristics, etc.).

At the same time, emerging ML-based approaches, like the ones described in the related work Section II, heavily rely on the availability of large quantities of performance monitoring (PM) data to train the cognitive tools responsible for QoT estimation. As discussed later in Section III, it becomes then important for each DM to be able to monitor alien wavelengths traversing the domain. In fact, these alien wavelengths are parts of the intra-domain traffic and should be considered when monitoring and learning from the real environment.

Manuscript received June xx 2018.

Roberto Proietti, Xiaoliang Chen, Kaiqi Zhang, Gengchen Liu, M. Shamsabardeh, and S. J. Ben Yoo are with the Department of Electrical and Computer Engineering at the University of California, Davis, USA (e-mail: rproietti@ucdavis.edu; xlichen@ucdavis.edu; sbyoo@ucdavis.edu).

Luis Velasco is with the Optical Communications Group (GCO) at Universitat Politècnica de Catalunya (UPC), Barcelona, Spain.

Alberto Castro was with University of California, Davis, USA at the time of this work. He is now with the Engineering School at the Universidad de la República, Montevideo, Uruguay.

Z. Zhu is with the School of Information Science and Technology, University of Science and Technology of China, Hefei, Anhui 230027, P. R. China (Email: zqzhu@ieee.org).

Roberto Proietti and Xiaoliang Chen equally contributed to the paper.

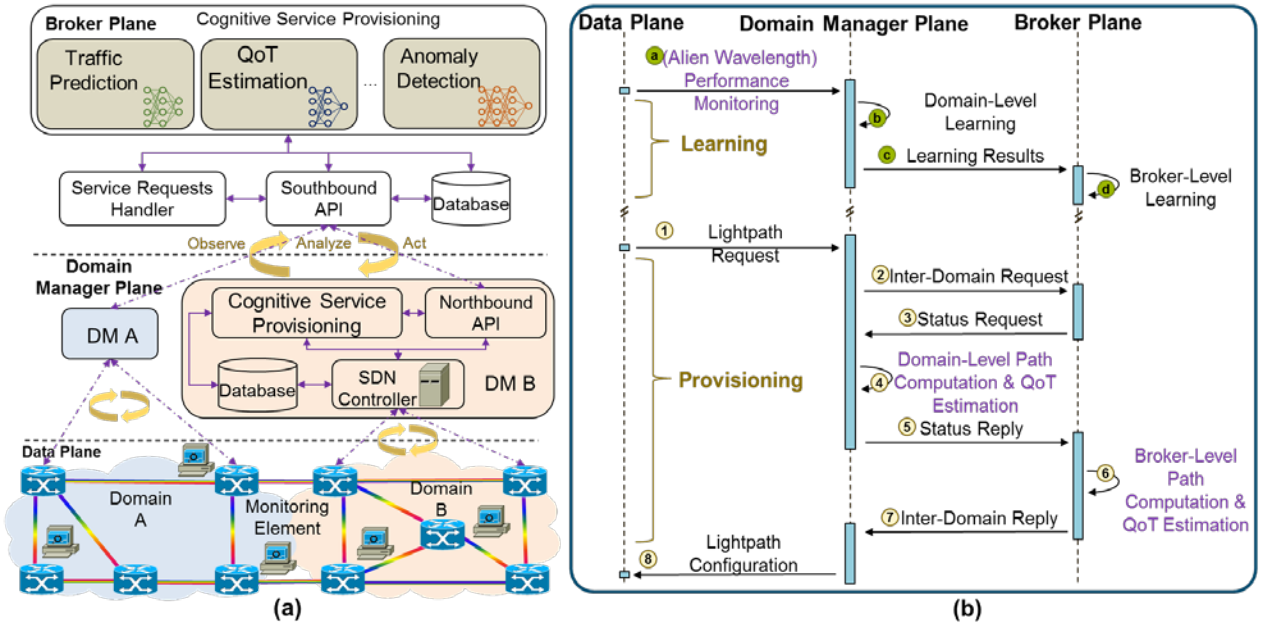

Fig. 1. (a) A schematic framework of the proposed cognitive multi-domain optical network with observe-analyze-act machine learning cycle and the broker plane interacting with the multiple domain managers. (b) The operation principle of the proposed framework.

In the context of a multi-domain network with orchestration [3], this paper extends the results published in [8], reporting the details regarding the alien wavelength PM technique (Section IV), as well as a new section with results on machine learning QoT estimation using a dataset from an experiment testbed (Section V.B). Overall, the main contributions of this paper are the following. First, we propose to use per-domain alien wavelength PM to assist ML-based QoT estimation in each domain. Second, we report a proof-of-concept experimental demonstration of alien wavelength PM by a combination of modulation format identification (MFI) [9] and supervisory channel (SC) techniques [10]. Third, we use datasets collected from an experimental testbed to demonstrate accurate training and QoT OSNR estimations using an ML approach based on *artificial neural networks* (*ANN*). Finally, we use a testbed to demonstrate a use case example of cognitive RMSA.

The remainder of this paper is organized as follows. Section II discusses the related work on cognitive optical networking with machine learning. Section III introduces the framework of the multi-domain network architecture with per-domain cognitive function and broker-based orchestration. Section IV introduces the working principle of the proposed alien wavelength PM technique. Section V reports the testbed experiments. Section VI concludes the paper.

II. Related Work

There has already been a significant amount of work on cognitive optical networking [11-14] and related applications of ML tools. For a comprehensive overview of the application of ML in optical networks, the readers can refer to [15, 16]. Below we briefly discuss a few papers grouped into three different categories: resource allocation, QoT estimation, and anomalies detection.

Cognitive resource allocation schemes: In [17], the authors implemented a neural network to facilitate adaptive bandwidth allocations in passive optical networks for ensuring users' quality-of-service. The authors of [18] proposed the use of ML for accurate blocking probability estimation of optical networks. In [19], Liu et al. proposed to incorporate neural network-based traffic prediction in the design of survivable IP-over-EONs so that resource bottlenecks can be avoided for potential future failure restorations. In [20], the authors reported a machine learning assisted resource orchestration scheme for optical datacenter networks, which can adapt the datacenter topology configurations dynamically based on the predicted application demands. More recently, we introduced data analytics to service provisioning of multi-domain EONs and demonstrated a knowledge-based framework for autonomous inter-domain traffic engineering [21].

Cognitive QoT estimation schemes: The authors in [22] proposed the use of machine learning (ML) techniques to estimate whether a given Routing,

Modulation format, and Spectrum Assignment (RMSA) would meet the desired QoT. Their approach consisted of training a classifier using a large dataset with measures obtained over the time. Here, the classifier should be periodically re-trained to reduce deviations by constantly collecting and storing the monitored data. A different approach was presented in [23], where the authors proposed to continuously monitor the optical layer and use such data to tune an analytical impairments model used for QoT estimation. In [24], the authors demonstrated a single domain ML-based optical signal to noise ratio (OSNR) predictor in an SDN network.

Cognitive anomaly/QoT degradation detection schemes: Ref. [25] analyzed several failure scenarios affecting the quality of optical connections and proposed two algorithms for detecting significant bit-error-rate changes and identifying failure patterns. The authors of [26, 27] discussed various types of real-life network fault use cases and proposed a variation based proactive fault detection scheme which was shown to be more efficient than the traditional threshold-based schemes. In [28], Shahkarami et al. compared different machine learning algorithms, i.e., support vector machine, random forest and neural networks, in performing anomaly detection and identification and discussed the trade-off between model accuracy and complexity for different methods. In [29], we leveraged hybrid unsupervised and supervised machine learn approaches and proposed a self-taught anomaly detection framework, which could detect unseen anomalies by learning patterns from monitoring data itself.

Nevertheless, existing works did not consider the multi-domain scenario with alien wavelengths, which requires careful studies of complex cases involving multiple ASes working cooperatively with limited information exchange.

III. Network Architecture

A. Cognitive Multi-Domain EON Architecture with Alien Wavelengths

Fig. 1(a) shows a schematic framework of the proposed cognitive multi-domain EON, which operates according to an ***Observe-Analyse-Act*** *cycle* [4]. The data plane of each EON domain contains bandwidth-variable transponders (BVTs) and bandwidth-variable wavelength selective switches (BV-WSSs). PM elements are deployed at certain locations for collecting the network status in real time (***Observe***). For instance, a coherent receiver can measure and report the bit-error-rate (BER) of an active connection. Also, SC PM tools can be used in each domain to monitor QoT (BER or OSNR) of alien wavelengths.

Note that the significance of monitoring alien wavelengths is two-fold. First, the state of alien wavelengths affects the performance of intra-domain connections. Second, such information enables better perceptions of the inter-domain traffic behavior, facilitating potentially better intra-domain planning result. DMs apply the software-defined networking (SDN) paradigm to operate their EON domains [30]. Specifically, SDN controllers residing in the domain control and management plane can collect PM data and conduct service provisioning by interacting with SDN agents that collocate with optical devices. Based on traffic engineering metrics and the received PM data, DMs can realize domain-level cognitive service provisioning. For instance, by analyzing the correlation between the path configurations and QoT, DMs may accurately predict the QoT of candidate RMSAs solutions (***Analyse***) and therefore, set up connections with guaranteed QoT and reduced margins (***Act)***.

A broker plane on top of DMs coordinates the service provisioning across multiple domains. The broker plane operates similarly to a DM, but only perceives limited or even no intra-domain information due to the administrative constraints in multi-AS systems. DMs can abstract their domains as virtual topologies consisting of virtual links among edge nodes [31] and report the QoT estimations of the virtual links as well as PM data of alien wavelengths measured at each of the edge nodes. Then, by utilizing a hierarchical learning approach [32, 33], multi-domain service provisioning with QoT assurance can be achieved.

B. Operation Principle

We summarize the operation principle of the proposed cognitive multi-domain EON framework with alien wavelength PM in the workflow in Fig. 1(b). Each DM constantly conducts PM for both intra-domain connections and alien wavelengths. A domain-level learning process is then executed (*step a*). The learned results can either be used for intra-domain provisioning (*step b*) or sent to the broker plane for learning the performance of inter-domain end-to-end lightpaths (*steps c-d*).

In the provisioning phase, upon receiving a lightpath request (*step 1*), the DM first determines whether it is for intra- or inter-domain transmission. If it is an intra-domain request, the DM immediately tries to calculate an RMSA solution that satisfies the QoT requirement. Specifically, the DM can calculate several candidate paths using an RMSA. Then the DM call the domain-level QoT estimation model to estimate the QoT of each candidate path solution provided by the RMSA. The QoT of existing in-service connections, in the case that each specific candidate RMSA is used, will also be evaluated.

The DM will choose the RMSA solution that satisfies the QoT requirement and ensures the QoT of existing connections. On the other hand, if the request is for inter-domain communication, the request is forwarded to the broker plane (*step 2*). To calculate an inter-domain lightpath, the broker plane requests for intra-domain information from the related DMs (*step 3*). Each involved DM, in turn, replies with several intra-domain candidate lightpaths together with their estimated QoT (*steps 4 and 5*). The broker plane aggregates the received data, builds a multi-domain virtual topology, and calculates an inter-domain end-to-end RMSA with QoT guarantee relying on the broker-level QoT estimation model (*step 6*, with a hierarchical learning approach [32, 33]). Finally, each related DM sets up the path segment within its domain to accomplish the inter-domain provisioning service (*step 8*).

IV. Alien Wavelength Monitoring System

As mentioned above, PM of alien wavelengths is essential for correct estimation of QoT parameters in intra- and inter- domain lightpath provisioning. In this section, we discuss the details of an alien wavelength PM system that can be used by the domains to identify the modulation format and OSNR of the alien lightpath traversing the domains. The proposed PM system exploits a combination of two monitoring techniques which are experimentally demonstrated in the subsequent sections. This PM system will be used at the ingress and the egress nodes of a domain, as shown later in Section V.

A. Supervisory Channel

The first PM tool is called supervisory channel (SC). Ref. [10] reported this technique for QPSK signals. In this paper, we extend the demonstration for the first time to QAM signals as well.

Fig. 2(a) shows the experimental setup used to evaluate and characterize the proposed PM technique. A standard coherent Tx (Co-Tx) consists of an external cavity laser (ECL), an *I/Q* modulator, and an electrical arbitrary waveform generator (EAWG) generating an optical M-QAM signal at 10 GBd. As part of the monitoring system, the optical signal is then fed into a second Mach-Zehnder modulator (MZM) to over-modulate the coherent signal with a 200 Mb/s ASK signal with 0.1 modulation index. Before the Rx (or at an intermediate node in the network where monitoring is needed), 10% of the optical power is tapped to the PM system, whereas the rest goes into a coherent receiver operating at full speed. The PM system consists of an avalanche photodiode (APD) and an analog low-pass filter (LPF) with 200 MHz bandwidth. An FPGA-based bit error rate tester (BERT) receives the ASK signal and calculates its BER and *Q*-factor.

Fig. 2(b) depicts the optical signal captured by the real-time oscilloscope (RTO). It shows that the low-speed ASK signal has shaped the envelope of the M-QAM signal. Fig. 2(c) and (d) present the waveform of the signal after the APD and LPF, respectively, clearly showing that the ASK symbols can be extracted from the high-speed M-QAM signal thanks to the LPF.

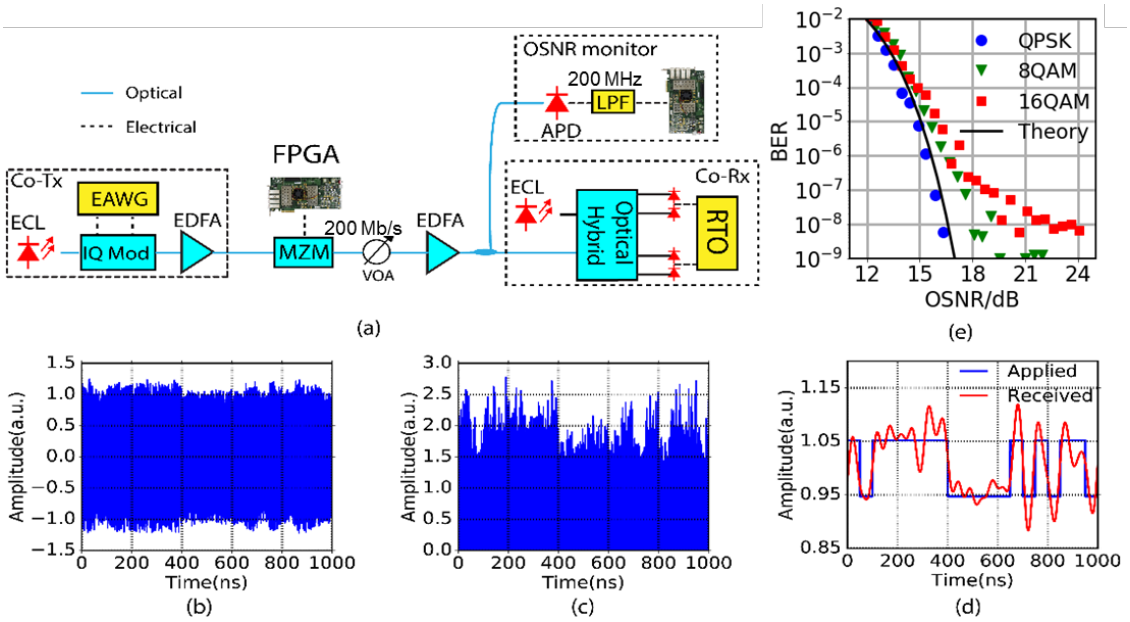

Fig. 2. (a) Experimental setup for characterization of the proposed technique. (b) 10 GBd 16-QAM waveform with ASK overmodulation. (c) Electrical waveform after the APD. (d) Received ASK signal after low-pass filtering (red curve; blue curve is the applied ASK signal at the transmitter). (e) Measured correlation curve between the Q-factor of the ASK signal and the OSNR for 4-QAM, 8-QAM, and 16-QAM.

We varied the OSNR values using a variable optical attenuator (VOA) and erbium doped fiber amplifier (EDFA) as noise loader. We measured the *Q*-factor of the ASK signal when the modulation format of the high-speed optical signal is QPSK, 8-QAM, and 16-QAM. An optical spectrum analyzer (OSA) with 0.1 nm resolution bandwidth is placed before the coherent receiver to measure the OSNR independently.

Fig. 2(e) shows the measured BER of the ASK signal with respect to the real OSNR measured by the OSA. When OSNR is relatively low, the BER is monotonically decreasing with OSNR. When the OSNR is greater than 20 dB, the BER experiences a floor due to the perturbation of the multi-level QAM signals on the ASK signal. Fig. 2(e) also shows the theoretical curve for reference. At high OSNR values, results from both modulation formats deviate from the theoretical model. We attribute this deviation to the amplitude fluctuation induced by the high-speed M-QAM signal. By recording the measured BER of the ASK signal and knowing the modulation index of the ASK signal and modulation format of M-PSK or M-QAM signal, low-cost OSNR and BER monitoring of the high-speed M-PSK and M-QAM signals can be achieved.

B. Modulation Format Recognition

As reported above, the SC technique allows monitoring QoT parameters (e.g., OSNR and BER) of an alien wavelength under the assumption that the modulation format is known.

However, in a multi-domain architecture, as described in Section II, the DM might not have access to this information, and therefore, a system that allows identifying the modulation format of alien wavelengths is needed to be able to use the PM systems proposed in the previous subsection. Such modulation format recognition system can serve other purposes like training of ML-based QoT estimators.

In Ref. [9], we already experimentally demonstrated a PM technique based on a blind modulation format identification (MFI) method. This technique can deliver very high accuracy (> 99%), even when the OSNR of the incoming signal is < 10 dB. The MFI technique allows identifying the modulation format by sampling the signal, performing a Fast Fourier Transform (FFT) of the samples after different power operations, and finally observing the peak to average ratio of the Fourier transform. Fig. 3 reproduces simulation results from [9] for the sake of completeness; the 512-point FFT after the nonlinear power transformations for different modulation formats are shown. The signals' baud rate was 10 GBd, and the laser linewidth was 100 kHz. After the correct power operation, a peak tone showed up in the signal's frequency spectrum.

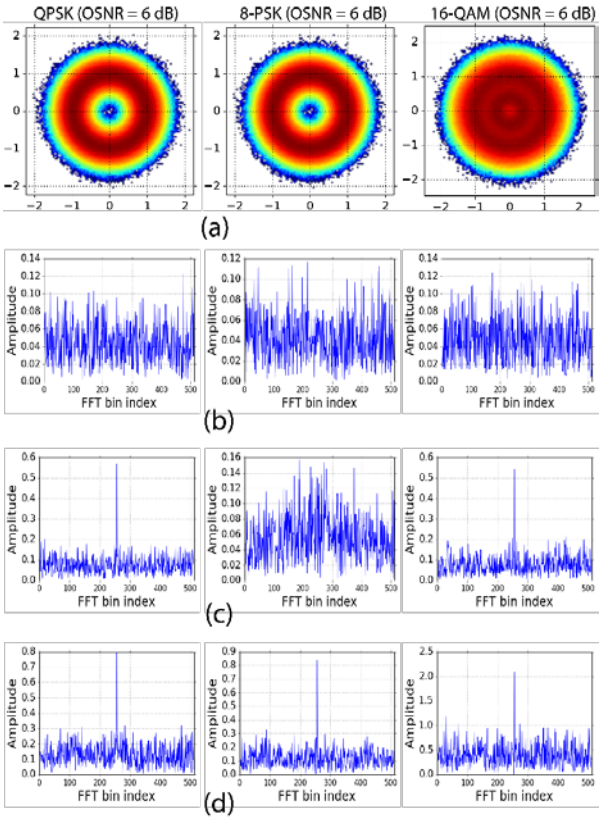

Fig. 3. (a) Constellation diagrams. (b) FFT after $(\,)^2$. (c) FFT after $(\,)^4$. (d) FFT after $(\,)^8$. [9]

By evaluating whether there is a peak tone or not after certain transformations and comparing the peak tone intensity against predefined threshold values (i.e., see the peak intensity difference between QPSK and 16QAM in Fig. 3(d), the MFI technique can determine the signals' modulation formats. Experimental studies reported in [9] demonstrated that the proposed MFI method could achieve successful identification rate as high as 99% when the incoming signal OSNR is as low as 7 dB. The reader can refer to ref. [9] for more details.

V. Testbed Experiments

The goal of the experimental testbed demonstrations discussed in the following section is threefold. First, Section V.A shows a proof of concept demonstration of alien wavelength monitoring by a combination of MFI and SC techniques. Second, in Section V.B, we demonstrate the use of experimental data to train a QoT OSNR estimator using an ML approach based on ANNs. Finally, Section V.C shows a simple use case scenario of cognitive RMSA; the scenario illustrates how the use of a legacy RMSA could lead to underestimating the physical impairments (saturation and noise loading conditions in the optically-amplified links), resulting in a connection failure due to excessively high BER at the receiver.

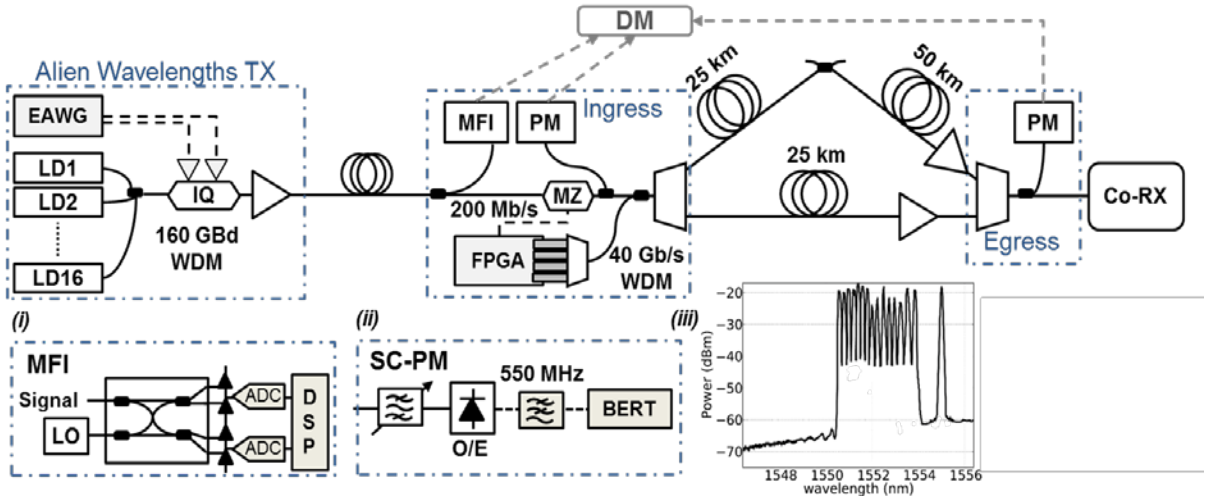

Fig. 4. Testbed. LD: laser diode; IQ: phase/quadrature modulator; MZ: Mach Zehnder modulator; DM: domain manager; Inset *(i)*: MFI monitoring: LO: local oscillator; ADC: analog to digital converter; DSP: digital signal processing; Inset *(ii)*: SC-PM monitoring: BERT: bit error rate tester; Inset *(iii)*: Alien wavelengths spectrum.

A. *Alien Wavelength Monitoring Experiment*

Fig. 4 shows the experimental testbed. An EAWG produces the analog electrical signals to generate QPSK or 8PSK alien wavelength signals and an *I/Q* block modulates 16 WDM lasers at 10 GBd (160 GBd). After the alien signals are amplified by an EDFA, they travel toward their destination network domain. The ingress node has PM capabilities based on MFI and SC (see also Section IV). The ingress node applies a low-speed (200 Mb/s) low-modulation-depth SC on the alien wavelengths to enable PM without significantly affecting the signals themselves. Insets *i)* and *ii)* in Fig. 4 show the schematic of MFI and SC-PM blocks (please refer to Section IV and also to [9] for more details). At the ingress node, an FPGA generating four WDM 10Gb/s signals acts as an intra-domain traffic source. There are two paths to reach the egress node with lengths of 25km and 75km, respectively. A PM block located at the egress node monitors the QoT of the alien signals going out of the domain.

Fig. 5 (a-b) show the results of the MFI monitoring block when changing the alien wavelength modulation format. For QPSK, Fig. 5(a) shows that after the power of four transformation, a peak can be observed in the FFT spectrum, which allows determining that the signal modulation format is QPSK.

When switching the modulation format to 8PSK, the peak in the FFT spectrum disappeared (see Fig. 5(b)); this allowed determining that the modulation format was 8PSK. Table I shows the results of SC monitoring at the ingress and egress nodes when the alien lightpath is modulated with QPSK and 8PSK and going through the shortest path.

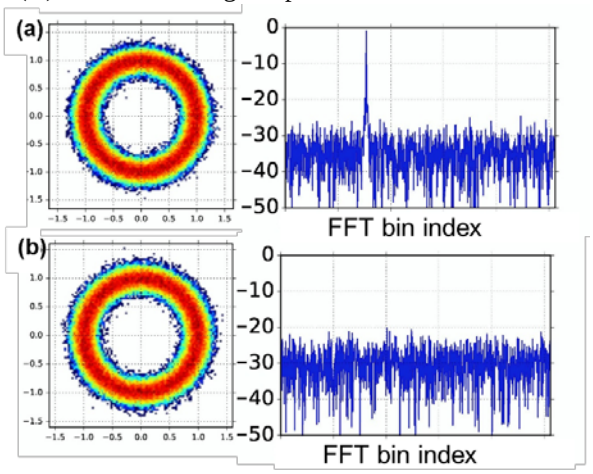

Fig. 5. MFI output for (a) QPSK and (b) 8PSK signals.

Table I. BER values in the testbed at Ingress and Egress nodes.

	QPSK/8PSK	
	Ingress	**Egress**
SC-BER	1E-3	3E-3
Alien λ OSNR	13.5 dB	12.7 dB

B. *ML-aided QoT Estimator Experiment*

Applying the alien wavelength PM technique, we demonstrated alien wavelength monitoring using the testbed of Fig. 4. In this section, we want to demonstrate instead an ANN-based tool to estimate the OSNR of unestablished lightpaths given the current network traffic conditions (traffic can be a combination of intra-domain traffic and alien wavelengths). Targeting a more realistic network scenario, we extended the experimental setup in Fig. 4 to a seven-node testbed, like the one reported in

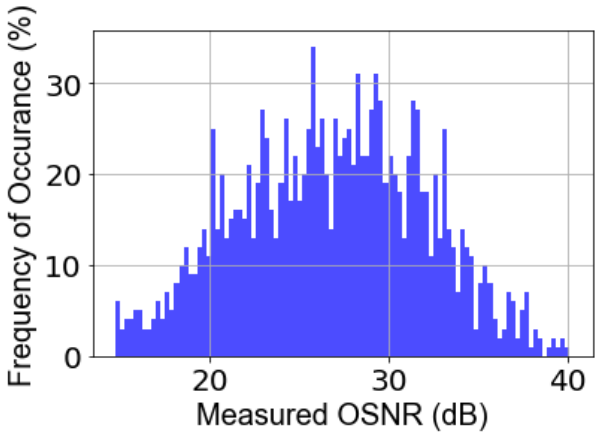

Fig. 6. OSNR distribution of the measured data.

Ref. [32] but assuming all the nodes belonging to the same domain. By regulating the routing paths and link loads of the testing lightpaths, we obtained 1,200 PM datasets to be used for training and testing purposes. Fig. 6 plots the histogram that shows the distribution of the measured OSNR for the target lightpaths.

The OSNR estimator makes use of an ANN consisting of two hidden layers. Fig. 7 shows the detailed structure of the OSNR estimator. The estimator takes as inputs the power measurements of all the channels together with the noise level on each link along the routing path to predict the OSNR of an end-to-end lightpath. Specifically, we set the length of the inputs as $L(N+1)+N$ to accommodate the monitoring data from all the links at the current time plus an indicator of N bits representing which of the channels will be used by the lightpath, where L and N denote the number of fiber links in the EON and the number of channels on each link, respectively. We encode the information of routing path setting all the bits corresponding to links that do not belong to the path as 0.

Each node j in layer i ($i > 1$) is fully connected to the nodes in layer $i-1$, and with an activation function $f(x) = \max(x, 0)$ [34], its output value is computed as,

$$h_{i,j} = f\left(\boldsymbol{w}_{i-1,j}^{T}\boldsymbol{h}_{i-1} + b_{i-1,j}\right),$$

where $\boldsymbol{w}_{i-1,j}$ contains the weights of the edges between node j and the nodes in layer $i-1$, and $b_{i-1,j}$ is the bias.

Here, we can see that node j is a higher-level representation of the nodes in the lower layer. Therefore, with multiple hidden layers, we can potentially extract the most useful features from the initial input data for the final OSNR estimation. The estimator is trained using the back-propagation method to fine-tune the values of $\boldsymbol{w}_{i-1,j}$ and $b_{i-1,j}$ such that the difference between the outputs of the ANN and the real monitoring OSNR is minimized. Eventually, we can infer the BER of lightpaths with the estimated OSNR according to the mappings in Fig. 2(e).

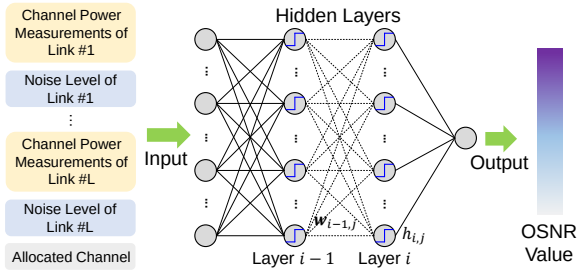

Fig. 7. Structure of the OSNR estimator.

Aiming at finding the right configuration of the ANN and the impact of the size of the training dataset on the performance of the OSNR estimator, we evaluate the prediction error for different numbers of nodes per layer and different sizes of training dataset (denoted as N) and plot the results in Fig. 8. Specifically, we randomly picked out certain numbers of data points from the whole dataset, divided them into the training and testing datasets with a proportion of 9:1, repeated the experiment for five times and calculated the average estimation errors. The estimation error is defined as $\frac{|O_{rel}-O_{est}|}{O_{rel}}$, where O_{rel} and O_{est} stand for the measured and estimated OSNR values (in linear scale), respectively. As expected, we can observe that the estimation accuracy improves with the number of data points since the estimator can learn more accurately the inherent correlations between the path performance and network configurations with more data. Meanwhile, we can see that the performance of the OSNR estimator improves significantly when the number of nodes in each layer is increased from 5 to 10 and then stays almost unchanged when the scale of the ANN further enlarges. Such observation indicates that under our specific experiment testbed setup and for the OSNR estimation task, two hidden layers with 10 nodes in each layer are sufficient for relatively good estimation accuracy.

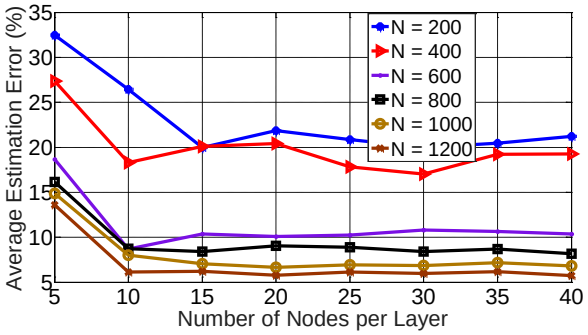

Fig. 8. Results on average prediction error.

Note that, we have also evaluated the impact of the number of hidden layers on the estimation accuracy and

the results show that two hidden layers are sufficient for the current dataset. This is because further adding the number of layers would lead to overfitting and thus bias the performance of the estimator.

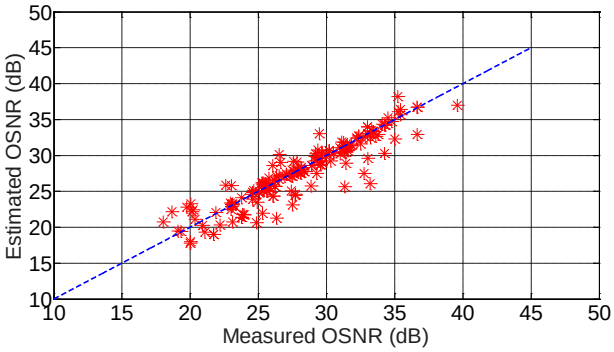

Fig. 9. Comparison between measured and estimated (red stars) OSNR.

Overall, with 1,200 data points and 40 nodes in each layer, the estimator can achieve an average estimation error of as low as 5.8%. It is reasonable to expect that the estimation accuracy will further improve when larger datasets are employed.

Finally, Fig. 9 shows the comparison between the measured OSNR values and the estimated ones when the size of the dataset is 1,200, which exhibits a good match and further verifies the practicability of the proposed method.

C. *Cognitive RMSA example.*

It is important to demonstrate that the use of a simple RMSA without cognitive functions could lead to underestimating the physical impairments (saturation and noise loading conditions in the optically-amplified links), resulting in a connection failure due to insufficient BER at the receiver. To this aim and to motivate our proposal, we performed a simple use case experiment on the testbed in Fig. 4. Let us assume that there is a 480 Gb/s alien lightpath request ***A*** (e.g., 8PSK modulation format) that must traverse the domain in the testbed. There is also a WDM lightpath ***B*** **(**40 Gb/s) currently established through link 1-3, which is already saturating the amplifier. In a scenario with simple RMSA, the network control plane could decide to route the request through link 1-3 (shortest path) using 8PSK modulation format [see Fig. 10(left)]. However, because the link is already loaded by intra-domain traffic, the QoT at the egress node might not be as expected (OSNR is too low and the estimated BER is 2.5E-2 (see Table II), which is higher than the 20%-FEC limit of 1.5E-2 [35]). Assuming instead that the network control plane has cognitive functions, it would use the information provided by the ML-aided OSNR estimator to consider the current link status and decide to route the 420 Gb/s alien signal through the longer but empty link 1-2-3 [see Fig. 10(right)]. As shown by the BER Table II, in this case, the BER at the egress node is below the pre-FEC BER limit.

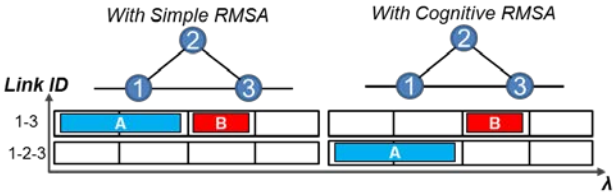

Fig. 10. (Left) Links status with simple RMSA. (Right) Links status with Cognitive RMSA.

Table II. BER values in the testbed at Ingress and Egress nodes. SC: supervisory channel; AW: alien wavelength.

	Simple RMSA		***Cognitive RMSA***	
	SC BER	**AW BER**	**SC BER**	**AW BER**
Ingress	1E-3	8.7E-4	1E-3	8.7E-4
Egress	8E-3	2.5E-2	2.7E-3	5.2E-3

VI. Conclusion

This paper experimentally demonstrated alien wavelength PM for cognitive provisioning in multi-domain networks. Each autonomous system (domain) makes use of optical PM to train an ANN-based QoT estimator to predict the OSNR of intra- and inter-domain lightpaths and make sure that the new connection to be established, as well as the existing ones, will meet the QoT requirements that guarantee BER values below the pre-FEC threshold.

By using *experimental data*, (a) we demonstrated a new monitoring technique for modulation format recognition and OSNR monitoring; (b) we trained an ANN-based ML QoT estimator capable to estimate the OSNR of a given lightpath with an estimation error < 6%; (c) we demonstrated a use case network scenario of cognitive routing based on the existing network conditions.

Future research works will focus on: (a) the use of larger testbeds to better understand how the estimation performance of the ML tool depends on the number of network nodes, the number of links, the size of the training datasets and specific ML approaches (e.g. Q-learning [36]); (b) hierarchical learning approaches for multi-domain routing [32].

ACKNOWLEDGMENT

This work was supported by DoE DE-SC0016700, AEI/FEDER TWINS (TEC2017-90097-R) grant, and ICREA Institution.

REFERENCES

[1] P. Poggiolini, "The GN model of non-linear propagation in uncompensated coherent optical systems," *Journal of Lightwave Technology*, vol. 30, pp. 3857-3879, 2012.

[2] Z. Zhu, C. Chen, X. Chen, S. Ma, L. Liu, X. Feng, and S. B. Yoo, "Demonstration of cooperative resource allocation in an OpenFlow-controlled multidomain and multinational SD-EON testbed," *Journal of Lightwave Technology*, vol. 33, pp. 1508-1514, 2015.

[3] A. Castro, L. Velasco, L. Gifre, C. Chen, J. Yin, Z. Zhu, R. Proietti, and S.-J. B. Yoo, "Brokered orchestration for end-to-end service provisioning across heterogeneous multi-operator (Multi-AS) optical networks," *Journal of Lightwave Technology*, vol. 34, pp. 5391-5400, 2016.

[4] S. Yoo, "Multi-domain cognitive optical software defined networks with market-driven brokers," in *Optical Communication (ECOC), 2014 European Conference on*, 2014, pp. 1-3.

[5] N. Skorin-Kapov, M. Furdek, S. Zsigmond, and L. Wosinska, "Physical-layer security in evolving optical networks," *IEEE Communications Magazine*, vol. 54, pp. 110-117, 2016.

[6] F. Cugini, N. Sambo, F. Paolucci, F. Fresi, and P. Castoldi, "Adaptation and monitoring for elastic alien wavelengths," in *Networks and Optical Communications (NOC), 2016 21st European Conference on*, 2016, pp. 82-87.

[7] I. Sartzetakis, K. Christodoulopoulos, C. Tsekrekos, D. Syvridis, and E. Varvarigos, "Quality of transmission estimation in WDM and elastic optical networks accounting for space–spectrum dependencies," *Journal of Optical Communications and Networking*, vol. 8, pp. 676-688, 2016.

[8] R. Proietti, X. Chen, A. Castro, G. Liu, H. Lu, K. Zhang, J. Guo, Z. Zhu, L. Velasco, and S. J. B. Yoo, "Experimental Demonstration of Cognitive Provisioning and Alien Wavelength Monitoring in Multi-domain EON," in *Optical Fiber Communication Conference*, 2018.

[9] G. Liu, R. Proietti, K. Zhang, H. Lu, and S. B. Yoo, "Blind modulation format identification using nonlinear power transformation," *Optics express*, vol. 25, pp. 30895-30904, 2017.

[10] D. J. Geisler, R. Proietti, Y. Yin, R. P. Scott, X. Cai, N. K. Fontaine, L. Paraschis, O. Gerstel, and S. Yoo, "Experimental demonstration of flexible bandwidth networking with real-time impairment awareness," *Optics express*, vol. 19, pp. B736-B745, 2011.

[11] G. S. Zervas and D. Simeonidou, "Cognitive optical networks: Need, requirements and architecture," in *Transparent Optical Networks (ICTON), 2010 12th International Conference on*, 2010, pp. 1-4.

[12] W. Wei, C. Wang, and J. Yu, "Cognitive optical networks: Key drivers, enabling techniques, and adaptive bandwidth services," *IEEE Communications magazine*, vol. 50, 2012.

[13] I. de Miguel, R. J. Durán, T. Jiménez, N. Fernández, J. C. Aguado, R. M. Lorenzo, A. Caballero, I. T. Monroy, Y. Ye, and A. Tymecki, "Cognitive dynamic optical networks," *Journal of Optical Communications and Networking*, vol. 5, pp. A107-A118, 2013.

[14] T. Jiménez, J. C. Aguado, I. de Miguel, R. J. Durán, M. Angelou, N. Merayo, P. Fernández, R. M. Lorenzo, I. Tomkos, and E. J. Abril, "A cognitive quality of transmission estimator for core optical networks," *Journal of Lightwave Technology*, vol. 31, pp. 942-951, 2013.

[15] F. Musumeci, C. Rottondi, A. Nag, I. Macaluso, D. Zibar, M. Ruffini, and M. Tornatore, "A Survey on Application of Machine Learning Techniques in Optical Networks," *arXiv preprint arXiv:1803.07976*, 2018.

[16] J. Mata, I. de Miguel, R. J. Durán, N. Merayo, S. K. Singh, A. Jukan, and M. Chamania, "Artificial intelligence (AI) methods in optical networks: A comprehensive survey," *Optical Switching and Networking*, 2018.

[17] N. Merayo, D. Juárez, J. C. Aguado, I. De Miguel, R. Durán, P. Fernández, R. Lorenzo, and E. Abril, "PID controller based on a self-adaptive neural network to ensure qos bandwidth requirements in passive optical networks," *Journal of Optical Communications and Networking*, vol. 9, pp. 433-445, 2017.

[18] H. C. Leung, C. S. Leung, E. W. Wong, and S. Li, "Extreme learning machine for estimating blocking probability of bufferless OBS/OPS networks," *Journal of Optical Communications and Networking*, vol. 9, pp. 682-692, 2017.

[19] S. Liu, B. Li, and Z. Zhu, "Realizing AI-assisted multi-layer restoration in a software-defined IP-over-EON with deep learning: An experimental study," in *Optical Fiber Communication Conference*, 2018, p. W4F. 1.

[20] W. Lu, L. Liang, B. Kong, B. Li, and Z. Zhu, "Leveraging predictive analytics to achieve

knowledge-defined orchestration in a hybrid optical/electrical DC network: Collaborative forecasting and decision making," in *Optical Fiber Communication Conference*, 2018, p. Th3F. 2.

[21] X. Chen, R. Proietti, H. Lu, A. Castro, and S. B. Yoo, "Knowledge-based Autonomous Service Provisioning in Multi-Domain Elastic Optical Networks," *IEEE Communication Magazine*, 2018.

[22] L. Barletta, A. Giusti, C. Rottondi, and M. Tornatore, "QoT estimation for unestablished lighpaths using machine learning," in *Optical Fiber Communications Conference and Exhibition (OFC), 2017*, 2017, pp. 1-3.

[23] S. Oda, M. Miyabe, S. Yoshida, T. Katagiri, Y. Aoki, T. Hoshida, J. C. Rasmussen, M. Birk, and K. Tse, "A learning living network with open ROADMs," *Journal of Lightwave Technology*, vol. 35, pp. 1350-1356, 2017.

[24] S. Yan, F. N. Khan, A. Mavromatis, D. Gkounis, Q. Fan, F. Ntavou, K. Nikolovgenis, F. Meng, E. H. Salas, and C. Guo, "Field trial of machine-learning-assisted and SDN-based optical network planning with network-scale monitoring database," in *43rd European Conference on Optical Communication (ECOC 2017)*, 2017.

[25] A. P. Vela, M. Ruiz, F. Fresi, N. Sambo, F. Cugini, G. Meloni, L. Potì, L. Velasco, and P. Castoldi, "BER degradation detection and failure identification in elastic optical networks," *Journal of Lightwave Technology*, vol. 35, pp. 4595-4604, 2017.

[26] D. Rafique, T. Szyrkowiec, H. Grießer, A. Autenrieth, and J.-P. Elbers, "Cognitive Assurance Architecture for Optical Network Fault Management," *Journal of Lightwave Technology*, vol. 36, pp. 1443-1450, 2018.

[27] D. Rafique, T. Szyrkowiec, H. Grießer, A. Autenrieth, and J. Elber, "TSDN-enabled network assurance: A cognitive fault detection architecture," in *Proc. Eur. Conf. Opt. Commun*, 2017.

[28] S. Shahkarami, F. Musumeci, F. Cugini, and M. Tornatore, "Machine-Learning-Based Soft-Failure Detection and Identification in Optical Networks," in *Optical Fiber Communication Conference*, 2018, p. M3A. 5.

[29] X. Chen, B. Li, M. Shamsabardeh, R. Proietti, Z. Zhu, and S. Yoo, "On Real-time and Self-taught Anomaly Detection in Optical Networks Using Hybrid Unsupervised/Supervised Learning," in *European Conference on Optical Communications*, 2018.

[30] X. Chen, M. Tornatore, S. Zhu, F. Ji, W. Zhou, C. Chen, D. Hu, L. Jiang, and Z. Zhu, "Flexible availability-aware differentiated protection in software-defined elastic optical networks," *Journal of Lightwave Technology*, vol. 33, pp. 3872-3882, 2015.

[31] X. Chen, Z. Zhu, L. Sun, J. Yin, S. Zhu, A. Castro, and S. Yoo, "Incentive-driven bidding strategy for brokers to compete for service provisioning tasks in multi-domain SD-EONs," *Journal of Lightwave Technology*, vol. 34, pp. 3867-3876, 2016.

[32] G. Liu, K. Zhang, X. Chen, H. Lu, J. Guo, J. Yin, R. Proietti, Z. Zhu, and S. B. Yoo, "The First Testbed Demonstration of Cognitive End-to-End Optical Service Provisioning with Hierarchical Learning across Multiple Autonomous Systems," in *Optical Fiber Communication Conference*, 2018, p. Th4D. 7.

[33] G. Liu, K. Zhang, X. Chen, H. Lu, J. Guo, J. Yin, R. Proietti, Z. Zhu, and S. J. Ben Yoo, "The First Testbed Demonstration of Cognitive End-to-End Optical Service Provisioning with Hierarchical Learning across Multiple Autonomous Systems," in *Optical Fiber Communication Conference Postdeadline Papers*, San Diego, California, 2018, p. Th4D.7.

[34] R. Arora, A. Basu, P. Mianjy, and A. Mukherjee, "Understanding deep neural networks with rectified linear units," *arXiv preprint arXiv:1611.01491*, 2016.

[35] D. Che, F. Yuan, and W. Shieh, "Maximum likelihood sequence estimation for optical complex direct modulation," *Optics Express*, vol. 25, pp. 8730-8738, 2017/04/17 2017.

[36] X. Chen, J. Guo, Z. Zhu, R. Proietti, A. Castro, and S. Yoo, "Deep-RMSA: A Deep-Reinforcement-Learning Routing, Modulation and Spectrum Assignment Agent for Elastic Optical Networks," in *Optical Fiber Communication Conference*, 2018, p. W4F. 2.